Electronic Supplementary Information

Constructing $CsPbBr_xI_{3-x}$ nanocrystal/carbon nanotube composite with improved charge transfer and light harvesting for enhanced photoelectrochemical activity

*Mu-Zi Yang,‡ Yang-Fan Xu,‡ Jin-Feng Liao, Xu-Dong Wang, Hong-Yan Chen and Dai-Bin Kuang**

MOE Key Laboratory of Bioinorganic and Synthetic Chemistry, Lehn Institute of Functional Materials, School of Chemistry, Sun Yat-sen University, Guangzhou 510275, P. R. China

***Email**: kuangdb@mail.sysu.edu.cn.

‡ These authors contribute equally to this work.

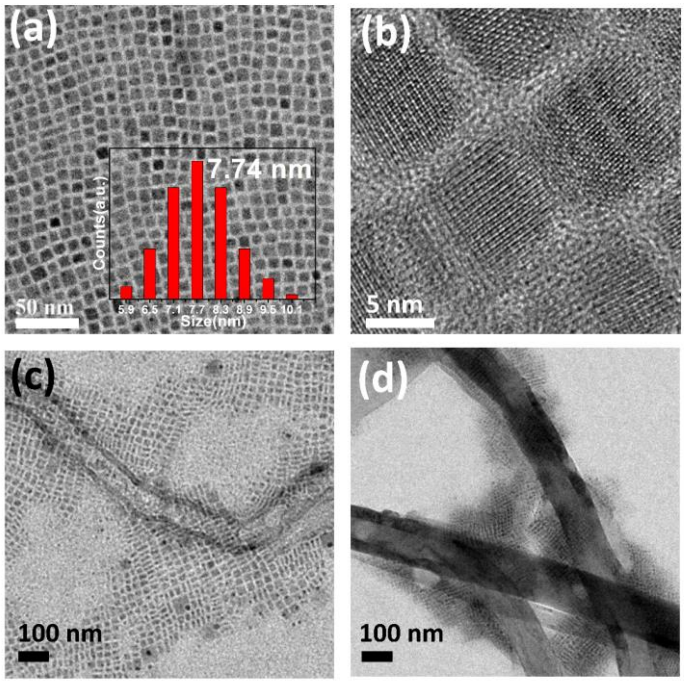

Fig. S1 TEM image of (a, b) the as-prepared $CsPbBr_3$ NC; (c) the $CsPbBr_3$ NC/CNT (100); (d) the $CsPbBr_3$ NC/CNT (400).

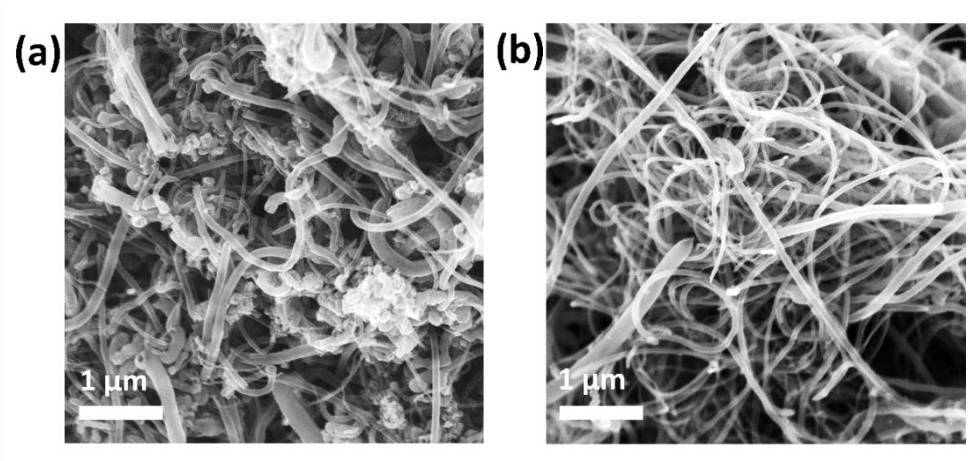

Fig. S2 The SEM images of CNTs (a) before and (b) after purification.

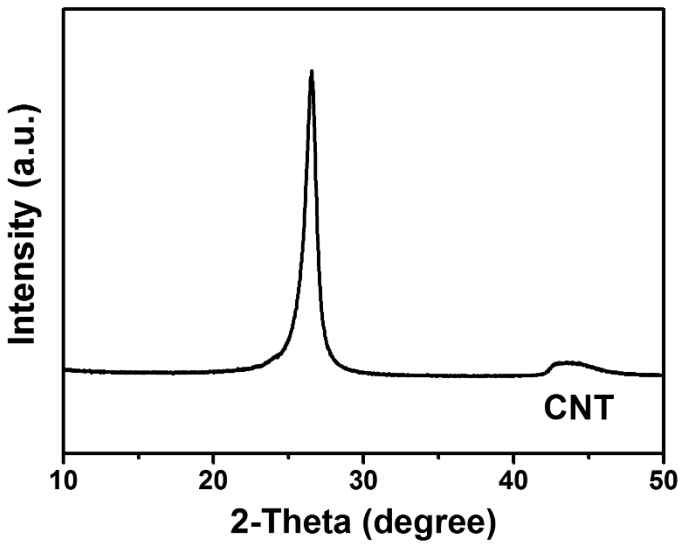

Fig. S3 XRD pattern of the purified CNT.

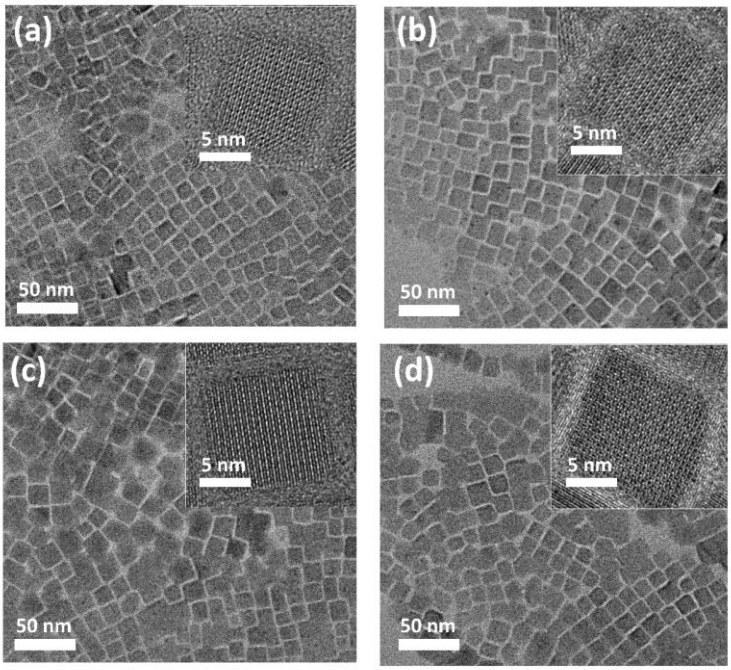

Fig. S4 The TEM images of $CsPbBr_xI_{3-x}$ NC: (a) $CsPbBr_2I$ NC (b) $CsPbBr_{1.5}I_{1.5}$ NC; (c) $CsPbBrI_2$ NC; (d) $CsPbI_3$ NC.

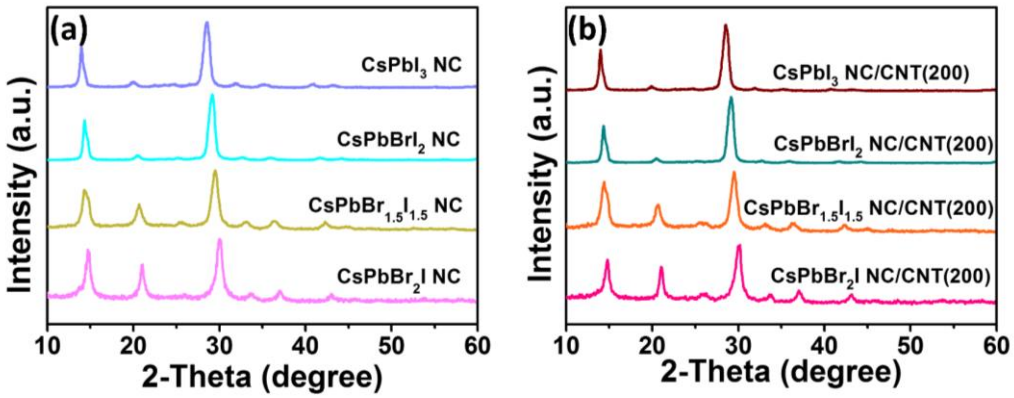

Fig. S5 The XRD patterns of (a) $CsPbBr_xI_{3-x}$ NC and (b) $CsPbBr_xI_{3-x}$ NC/CNT (200).

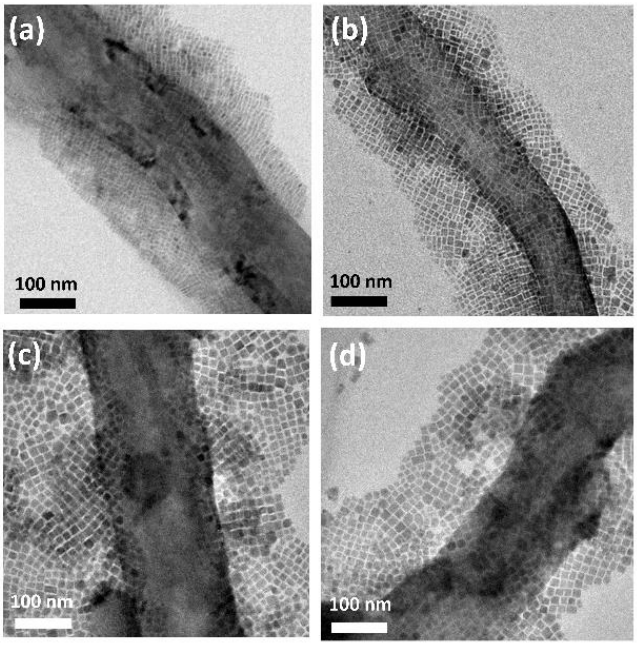

Fig. S6 The TEM images of (a) $CsPbBr_2I$ NC/CNT (200); (b) $CsPbBr_{1.5}I_{1.5}$ NC/CNT (200); (c) $CsPbBrI_2$ NC/CNT (200); (d) $CsPbI_3$ NC/CNT (200).

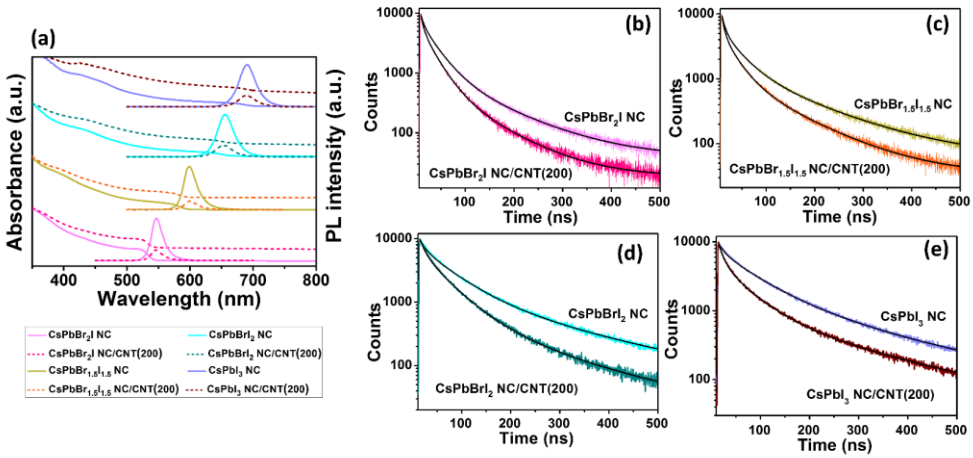

Fig. S7 (a) Absorption spectra and steady-state PL spectra of the $CsPbBr_xI_{3-x}$ NC and $CsPbBr_xI_{3-x}$ NC/CNT (200). (b-e) Transient-state PL spectra of the $CsPbBr_xI_{3-x}$ NC and $CsPbBr_xI_{3-x}$ NC/CNT (200), with an excitation wavelength of 369.6 nm.

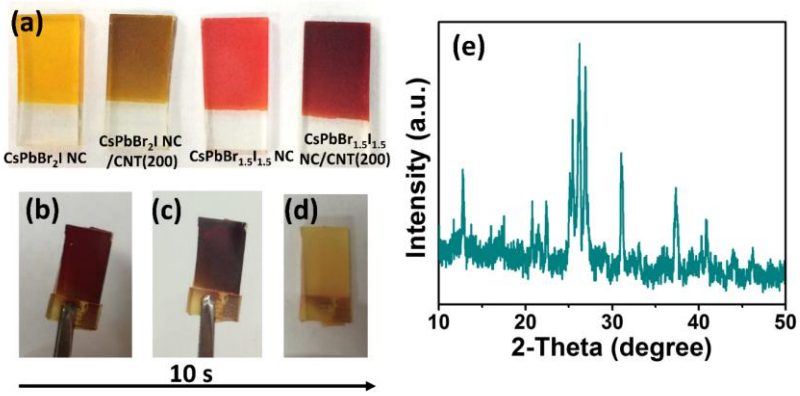

Fig. S8 (a) The photos of the $CsPbBr_xI_{3-x}$ NC and the $CsPbBr_xI_{3-x}$ NC/CNT (200) Films (x=2, 1.5), (b-d) Color-change process of the $CsPbBrI_2$ NC film in the air within 10 s. (e) the XRD pattern of the $CsPbBrI_2$ NC/CNT (200).

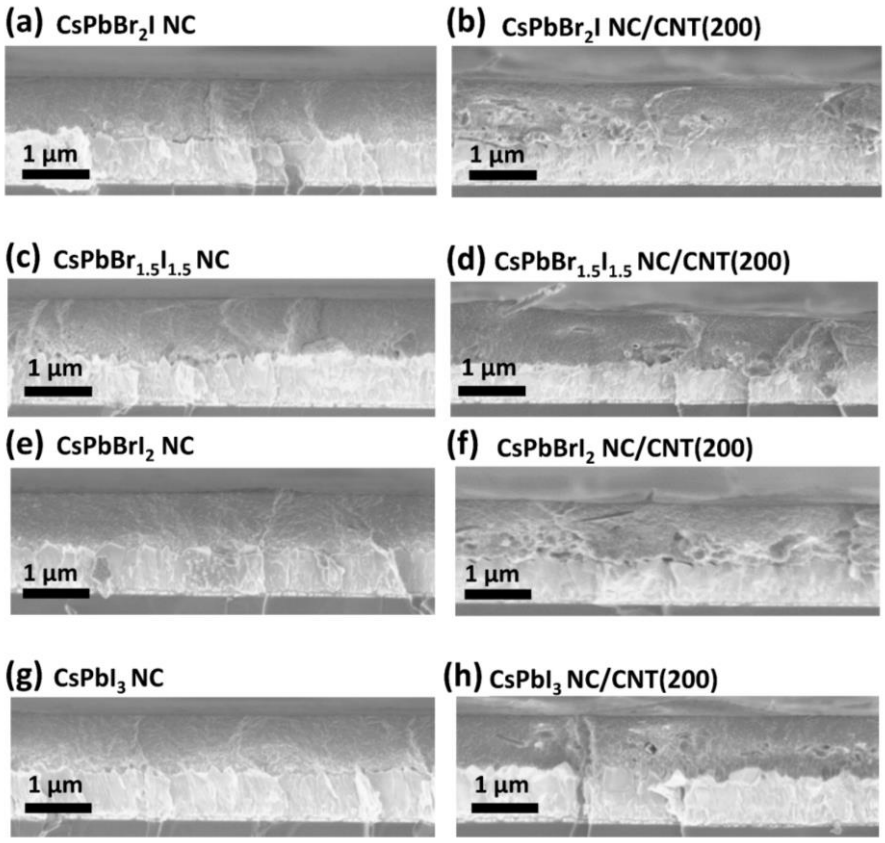

Fig. S9 The cross-section SEM images of the $CsPbBr_xI_{3-x}$ NC and $CsPbBr_xI_{3-x}$ NC/CNT (200) (x=0, 1, 1.5, 2).

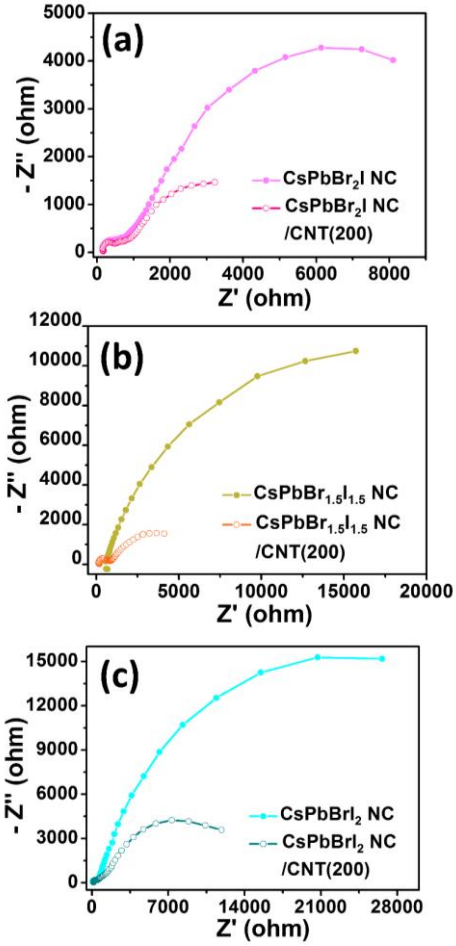

Fig. S10 EIS Nyquist plots of the $CsPbBr_xI_{3-x}$ NC and $CsPbBr_xI_{3-x}$ NC/CNT (200) (x=1, 1.5, 2) photoelectrodes. The tests are conducted under a bias of -0.4 V vs. Ag/AgCl. A 150 W Xe lamp with an AM 1.5G filter and 150 mW cm^{-2} was used as a light source.

Table S1. The specific volume ratio in fabrication of $CsPbBr_xI_{3-x}$ NC/CNT hybrids

Samples	$CsPbBr_xI_{3-x}$ colloid (in toluene)	CNT dispersion	Ethyl acetate
$CsPbBr_3$ NC	1000 μL	0 μL	
$CsPbBr_3$ NC/CNT(100)	900 μL	100 μL	
$CsPbBr_3$ NC/CNT(200)	800 μL	200 μL	1mL
$CsPbBr_3$ NC/CNT(400)	600 μL	400 μL	

Table S2. The specific data transient and steady photocurrent density of $CsPbBr_3$ NC and $CsPbBr_3$ NC/CNT hybrids

Samples	Transient-state photocurrent density of (μA/cm^2)	Steady state photocurrent density (μA/cm^2)
$CsPbBr_3$ NC	48.1	39.7
$CsPbBr_3$ NC/CNT(100)	128	83.2
$CsPbBr_3$ NC/CNT(200)	206	127
$CsPbBr_3$ NC/CNT(400)	84.8	50.5

Table S3. The TAS decay kinetics fitting results of $CsPbBr_3$ NC and $CsPbBr_3$ NC/CNT hybrids

Samples	τ_1 (ns)	τ_2 (ps)	Standard deviation
$CsPbBr_3$ NC	11.8	399	0.00124
$CsPbBr_3$ NC/CNT(100)	10.3	286	0.00091
$CsPbBr_3$ NC/CNT(200)	6.65	176	0.00126
$CsPbBr_3$ NC/CNT(400)	5.32	102	0.00118

Table S4. The specific transient and steady photocurrent densities of $CsPbBr_xI_{3-x}$ NC and $CsPbBr_xI_{3-x}$ NC/CNT hybrids

Samples	Photocurrent density of transient state (μA/cm^2)	Photocurrent density of steady state (μA/cm^2)
$CsPbBr_2I$ NC	88.7	58.8
$CsPbBr_2I$ NC/CNT(200)	273	186
$CsPbBr_{1.5}I_{1.5}$ NC	117	63.6
$CsPbBr_{1.5}I_{1.5}$ NC/CNT(200)	417	236
$CsPbBrI_2$ NC	63.5	36.2
$CsPbBrI_2$ NC/CNT(200)	177	127

Table S5. Summary of the average PL lifetimes for the $CsPbBr_xI_{3-x}$ NC and $CsPbBr_xI_{3-x}$ NC/CNT hybrids

Samples	$\tau_{average}$ / ns	χ
$CsPbBr_2I$	58.85	1.102
$CsPbBr_2I$ /CNT (200)	44.05	1.128
$CsPbBr_{1.5}I_{1.5}$	85.96	1.237
$CsPbBr_{1.5}I_{1.5}$/CNT (200)	62.63	1.077
$CsPbBrI_2$	124.19	1.417
$CsPbBrI_2$/CNT (200)	77.06	1.195
$CsPbI_3$	143.25	1.566
$CsPbI_3$/CNT (200)	118.16	1.482

Table S6. The EIS fitting results of $CsPbBr_xI_{3-x}$ NC and $CsPbBr_xI_{3-x}$ NC/CNT hybrids

Samples	Without CNT(ohm)	with 200 μL CNT(ohm)
$CsPbBr_2I$ NC	20037	7820
$CsPbBr_{1.5}I_{1.5}$ NC	31119	6419
$CsPbBrI_2$ NC	45874	18019